

Dynamical mechanical properties of polyvinylbutyral nanocomposites - A comparison between different nano-carbon reinforcements

Jean Carlos Hoepfner¹, Renato César Tobias Porto¹,
Patrícia Zigoski Uchôa¹, André Lourenço Nogueira²,
Sérgio Henrique Pezzin³

¹Santa Catarina State University (UDESC), Center of Technological Sciences, Paulo Malschitzki Street #200, Zip Code 89219-710 Joinville, Santa Catarina, Brazil;

²University of the Region of Joinville (UNIVILLE), Department of Chemical Engineering, Paulo Malschitzki Street #10, Zip Code 89219-710, Joinville, Santa Catarina, Brazil

³Santa Catarina State University (UDESC), Center of Technological Sciences, Department of Chemistry; Paulo Malschitzki Street #200, Zip Code 89219-710 Joinville, Santa Catarina, Brazil;

E-mail: hoepfner.jean@gmail.com, rctporto@hotmail.com, pzucho@hotmail.com, sergio.pezzin@udesc.br, andre.lourenco@univille.br;

ABSTRACT

In this work, the role of the degree of acetalization of polyvinylbutyral (PVB) on the dynamic mechanical properties of PVB nanocomposites was evaluated. Nanocomposites reinforced with carbon nanoparticles (pristine or oxidized multi-walled carbon nanotubes, graphene oxide and graphene nanoplatelets) were prepared by in situ addition during the synthesis of PVB from polyvinyl alcohol. It was found that the presence of nanoreinforcements during the synthesis considerably alters the degree of acetalization (AD) of PVB (ca. 65 mol% for the neat polymer), which values ranged from 50 to 77 mol%. Dynamic mechanical analyses were used to calculate the storage modulus and other parameters such as: factor C, degree of entanglement and adhesion factor, which were correlated with scanning electron microscopy images. There was a tendency to decrease AD with the increase in the degree of oxidation of the nanoreinforcements, however this contributed to a better dispersion and adhesion of these to the polymer matrix and, consequently, altered positively the nanocomposite properties.

Keywords: polyvinylbutyral, nanocomposites, carbon nanotubes, graphene nanoplatelets, dynamic mechanical analysis, acetalization degree.

1. INTRODUCTION

Polyvinyl butyral (PVB), which chemical structure is shown in Figure 1, is a random thermoplastic copolymer, transparent and resilient, used in various applications, from interlayers in glass sandwiches for automotive wind-shielding [1, 2] to ultrafiltration membranes [3], encapsulation of photovoltaic panels [4], adhesives [5, 6] and military components [7].

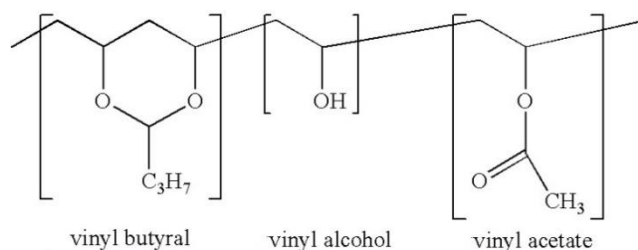


Figure 1: Structure of PVB containing butyral rings, hydroxyl and acetal groups.

The application of PVB is directly connected to its acetalization degree (AD) and, thus, the determination of its value is critical. [1] The interaction between hydrophobic (butyral groups) and hydrophilic (vinyl alcohol) moieties will generate a material with variations in thermal and mechanical strength, and thus the control of the AD in the PVB synthesis from polyvinyl alcohol (PVA) and butyraldehyde is well studied, [8-10]. Although the acetalization process is considered to be random and irreversible, generating hypothetically AD values up to 87 mol% [11], higher values can be obtained considering the non-random and reversible acetalization process, in which hydrolysis of butyral and acetal groups and condensation of adjacent hydroxyl groups can occur. [8]

However, there are few studies in the literature that report the influence of the AD in PVB nanocomposites, nearly all of them describing preparations involving the addition of nanoparticles to PVB solutions (so-called 'solution methods'). [12] Researching the influence of graphene oxide (GO) and graphene nanoplatelets (GNP) on the thermo-mechanical properties of PVB nanocomposites, Hoepfner et al. showed that the addition of nanoparticles *in situ*, i.e. during the PVB synthesis, can improve the dispersion and particle/matrix interaction. The study pointed out variations in AD among the samples, but it was not clearly indicated if the nanoparticles were responsible for such changes [13] In another work, the authors prepared PVB nanocomposites with nanoclay functionalized with 3-aminopropyltriethoxysilane, via 'in situ' polymerization, testing different concentrations of nanoclay and AD values. It was found that the best results of mechanical strength were observed for 4 wt% of nanoclay and 50 mol% AD. The authors commented that there were no changes in the AD values even with the addition of nanoclay. [14]

Carbon nanoparticles have been extensively used as reinforcements in composites, especially 'graphene' and multi-walled carbon nanotubes (CNT). [15] The term 'graphene' comprises several materials, constituted of carbon atoms with sp² hybridization forming hexagonal cells, ranging from a monolayer to sets of 10-20 stacked sheets named graphene nanoplatelets (GNP). [16] In addition to exceptional mechanical properties and outstanding electrical and thermal conductivities [17, 18] graphene structures present good transmittance (97.7% for a single layer), while CNT have distinguished aspect ratios, making them great candidates for applications in transparent conductive electrodes [19, 20] for solar cells and flexible touch displays. It is also known that a controlled oxidizing treatment [21, 22] generating carboxyl, hydroxyl and carbonyl groups attached to GNP and CNT surfaces, contributes to a better dispersion and polymer-nanoparticle adhesion. [23, 24]

Thus, in this work, we studied the influence of 'in situ' addition of pristine and oxidized carbon nanoparticles (GNP and CNT) on the acetalization degree of PVB and its dynamic mechanical (DMA) properties. The AD values, determined by proton nuclear magnetic resonance (¹H NMR), and nanocarbon concentrations have been correlated with DMA results and scanning/transmission electron microscopy images.

2. MATERIALS AND METHODS

Graphite was purchased from Labsynth (*São Paulo, Brasil*), with particle size <45 µm, 98% purity and 1.0% ash content. Multiwalled carbon nanotubes (MWCNT) were supplied by Chengdu Organic Chemicals (*Chengdu, China*) with a purity greater than 85%, with external diameter of 10-30 nm, internal diameter of 5-10 nm and length of 10-30 µm. Polyvinyl alcohol (PVA) with a molecular weight of 85.300 g mol⁻¹ was provided by *Vetec Chemistry* and butyraldehyde (BU) 98% by *Sigma-Aldrich*. Sulfuric acid 98% (*Cinética*), nitric acid 65% (Merck), hydrochloric acid 37% (*Cinética*), glacial acetic acid (*Cinética*), sodium lauryl sulphate (*Cinética*), sodium nitrate (*Synth*), potassium permanganate (*Synth*) and hydrogen peroxide 35% (*Cinética*) were used without prior treatments.

2.1 Preparation of PVB nanocomposites

Graphene oxide (GO) was produced from graphite using an adaptation of the Hummers method, as discussed elsewhere [25], while the oxidation of MWCNT was performed according to another study from our research group. [26].

Table 1: Compositions of PVP nanocomposites

Sample	Nanoparticle	Concentration wt%
PVB-MWCNT	Carbon nanotube	0.1; 0.5; 1.0
PVB-MWCNTO	Oxidized carbon nanotubes	0.1; 0.5; 1.0
PVB-GO	Graphene oxide	0.5; 1.0; 2.5
PVB-GNP	Graphene nanoplatelets	0.5; 1.0; 2.5

The synthesis of PVB, from PVA and butyraldehyde, and its nanocomposites (*in situ*) was adopted from the method developed by our research group and discussed elsewhere. [13] The nanoparticles were dispersed using a high end sonicator (Sonics 750 W) and added to a reaction vessel along with PVA, BU, sodium lauryl sulfate, deionized water, acetic acid and some drops of sulfuric acid. The system was kept for 2 hours in 10 °C, followed by a half hour at 70 °C. Finally, the PVB was precipitated with the addition of deionized water, washed, filtered, and dried to constant mass. The same procedure was used for all nanoparticles: graphene oxide (GO), graphene nanoplatelets (GNP), pristine carbon nanotubes (MWCNT) and oxidized carbon nanotubes (MWCNTO). However, in the case of pristine and oxidized MWCNT, concentration values ranged from 0.1 to 1.0 wt%, while for GO and GNP the values ranged between 0.5 and 2.5 wt% (Table 1). The specimens were prepared by pressing the samples in a hydraulic press under 2 Ton for 5 minutes at 160 °C, followed by cooling at room temperature.

2.2 Characterizations

Dynamic mechanical analyses (DMA) were recorded using a TA instrument model 2980 at a frequency of 2 Hz, heating rate of 5 °C min⁻¹, from 25 °C to 110 °C. AD values were obtained in previous works.[13, 27] Spectra were recorded using a 400 MHz Bruker Advanced spectrometer, using DMSO-d₆ as solvent, without internal standard. The analyses of the fracture surfaces of tensile-tested specimens were performed on a field-emission scanning electron microscope (FE-SEM) JEOL-6701F, after gold sputtering.

3. RESULTS AND DISCUSSIONS

4. 3.1 ACETALIZATION DEGREES

The values of acetalization degree (AD), corresponding to the vinyl butyral content, were calculated from previous studies [13, 27] by equation (1) where A_{CH₂} and A_{CH₃} are the total areas of methylene and methyl protons, respectively. [1] The calculated values of the acetalization degree are shown in Table 2.

$$(AD) = \frac{2}{\left(\frac{A_{CH_2}}{A_{CH_3}}\right)^{-6}} \quad (1)$$

Table 2: Acetalization degree (AD) values for PVB and composites with nanocarbons (from [13, 27]).

SAMPLE (wt%)	AD (mol%)
PVB	65
PVB-MWCNT 0.1	50
PVB-MWCNT 0.5	58
PVB-MWCNT 1.0	77
PVB-MWCNTO 0.1	68
PVB-MWCNTO 0.5	56
PVB-MWCNTO 1.0	55
PVB-GO 0.5	60
PVB-GO 1.0	68
PVB-GO 2.5	51
PVB-GNP 0.5	65
PVB-GNP 1.0	66

There are significant variations in the values of AD. In the case of samples reinforced with pristine MWCNT and GNP, the AD values increase linearly with the increase of the concentration of nanoparticles dispersed in PVB. For samples reinforced with oxidized nanocarbons, MWCNTO and GO, the AD values decrease with increasing concentration of the nanoparticles. This behavior indicates that oxidized nanoparticles, due to the presence of oxygenated groups, such as hydroxyls, hampered the condensation of butyraldehyde (BU) with the OH groups of PVA and, consequently, there was a decrease in the value of AD. The higher the amount of dispersed oxidized nanoparticles in PVB, the greater the probability of BU reacting with the oxygen groups of the nanoparticles. For the samples reinforced with pristine MWCNT and GNP an opposite behavior is observed, probably due to the formation of agglomerates of nanoparticles and absence of oxygen groups.

3.2 Dynamical Mechanical Analysis

Figure 2 compare dynamic mechanical curves for PVB and its nanocomposites from data reported in foregoing studies [13, 27], while Table 3 summarizes the values of storage modulus and their relation with AD.

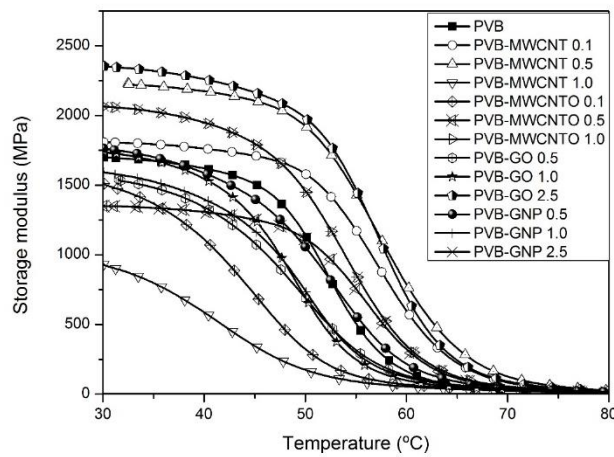


Figure 2: Curves of storage modulus for PVB and nanocomposites, obtained from [13, 27].

In the case of PVB-MWCNT 1.0 and PVB-MWCNTO 0.1 samples, there is a rapid decay of the modulus storage with temperature. This behavior is expected when PVB presents a high AD value, since the absence of hydroxyls in the polymer chain would prevent the formation of hydrogen bonds between the polymer chains, which would result in a less rigid material. [14] This result is in agreement with the calculated AD values, as observed in Table 3. On the other hand, for the PVB-GO 2.5 wt% sample, the high storage modulus value can be related to GO exfoliation and high concentration of nanoreinforcement.

When the variations in storage modulus values are compared, it is observed that the higher increases in storage modulus are related to the lower AD values. Yet, the sharpest decreases in storage modulus values are related to the highest AD values.

This analysis demonstrates two aspects: firstly, besides the effect of the nanoparticles, the AD also contributes significantly for the increase of storage moduli, especially for the samples with lower AD values, i.e. with chemical structures more similar to PVA. The other aspect is that the AD values have been influenced by the presence of the carbon nanoparticles.

Table 3: Values of the storage modulus at 30°C, respective % variation in relation to PVB, and values of AD for PVB and nanocomposite samples.

Sample	Storage Modulus (GPa)	Variation in relation to PVB (%)
PVB	1.70	---
PVB-MWCNT 0.1	1.80	6.0
PVB-MWCNT 0.5	2.21	30.0
PVB-MWCNT 1.0	0.98	- 43.5
PVB-MWCNT0 0.1	1.45	- 15.5
PVB-MWCNT0 0.5	1.34	- 21.2
PVB-MWCNT0 1.0	2.05	20.5
PVB-GO 0.5	1.53	-10.0
PVB-GO 1.0	1.72	1.1
PVB-GO 2.5	2.35	38.2
PVB-GNP 0.5	1.76	3.5
PVB-GNP 1.0	1.58	-7.6
PVB-GNP 2.5	1.74	2.3

To measure the efficiency of the reinforcement in the mechanical behavior of the nanocomposites, the C-factor was calculated by Equation (2) [28, 29] where $E'g$ and $E'r$ are the values of storage modulus in the glassy region (30 °C) and rubbery region (60 °C), respectively. The C-factor indicates the effective contribution of the nanoparticles in the transition from the vitreous to the rubbery state.

$$C = \frac{\left(\frac{E'g}{E'r}\right)_{composites}}{\left(\frac{E'g}{E'r}\right)_{pure}} \quad (2)$$

The greater the intermolecular forces, the more energy is required to this conversion; that is, the nanoparticles act in this process restricting the glass transition. The higher the efficiency of the nanoparticles, the more energy will be spent and the lower the C-factor [29] Table 4 correlates C-factor values with AD values and their respective samples. The C-factor values and its relationship with AD are summarized in Figure 3.

Table 4: C-factor and AD values for PVB and nanocomposite samples

Sample	C-factor	AD (mol%)
PVB	1	65
PVB-MWCNT 0.1	0.65	50
PVB-MWCNT 0.5	0.65	58
PVB-MWCNT 1.0	4.22	77
PVB-MWCNT0 0.1	3.75	68
PVB-MWCNT0 0.5	0.70	56
PVB-MWCNT0 1.0	0.87	55
PVB-GO 0.5	1.61	60
PVB-GO 1.0	1.78	68
PVB-GO 2.5	0.68	51
PVB-GNP 0.5	1.15	65
PVB-GNP 1.0	2.09	66
PVB-GNP 2.5	1.76	69

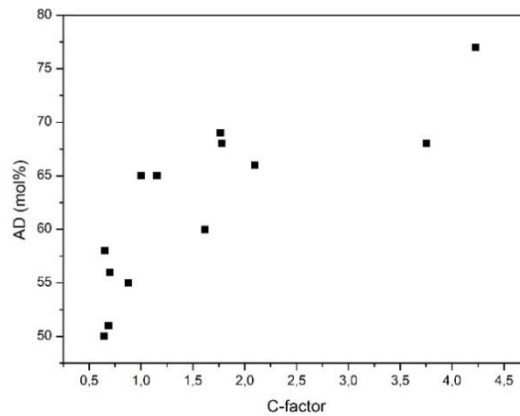


Figure 3: Relationship between C-factor and AD values.

It can be observed that the efficiency of the nanoparticles was higher for in the samples with the lowest AD values. For such nanocomposites, the C-factor values agree with the largest increases in the storage modulus, indicating that dispersion and nanoparticle/matrix interaction were relevant.

Another parameter studied was the degree of entanglement, 'N'. This parameter gives an estimation of the dispersion of the nanoparticles within the polymer matrix and can be calculated by the Equation (3) [29], where E' is the storage modulus, R is the universal gas constant, and T is the absolute temperature. The higher the value of 'N', the more dispersed are the nanoparticles into the polymer matrix. 'N' values lower than those obtained by the matrix itself indicate that the nanoparticles are agglomerated. [30] Yet, a high degree of entanglement denotes a valuable interaction between nanoparticles and polymer matrix. [31].

$$N = \frac{E'}{6RT} \tag{3}$$

Table 5 shows the correlates the degree of entanglement 'N' and AD values with the respective samples and PVB. Figure 4 presents show the relationship of the degree of entanglement ('N') and the AD values.

Table 5: Degree of entanglement ('N') and AD values for PVB and nanocomposite samples

Sample	'N'	AD (mol%)
PVB	0.011	65
PVB-MWCNT 0.1	0.012	50
PVB-MWCNT 0.5	0.015	58
PVB-MWCNT 1.0	0.006	77
PVB-MWCNT 0.1	0.009	68
PVB-MWCNT 0.5	0.009	56
PVB-MWCNT 1.0	0.014	55
PVB-GO 0.5	0.010	60
PVB-GO 1.0	0.011	68
PVB-GO 2.5	0.016	51
PVB-GNP 0.5	0.011	65
PVB-GNP 1.0	0.010	66
PVB-GNP 2.5	0.012	69

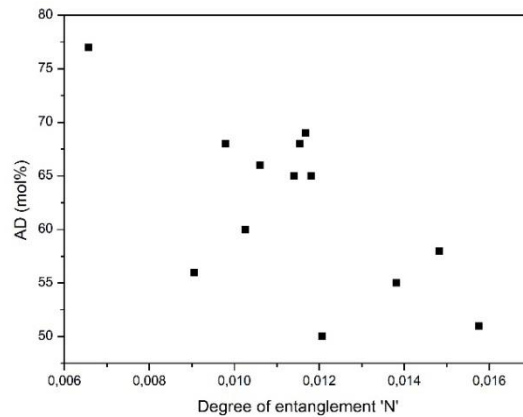


Figure 4: Relationship between degree of entanglement 'N' and AD values

It is noted that the highest 'N' values were also obtained for samples with lower AD values, indicating that the nanoparticles are better dispersed in systems where there is a greater amount of vinyl alcohol groups. This fact can be attributed to the presence of oxygenated groups in the oxidized samples and also in the pristine samples, which facilitate their interaction and dispersion in the polymer matrix. It is worth mentioning that it is in full agreement with the C factor values.

Tan δ curves from dynamic mechanical analyses are shown in Figure 5 and T_g values are summarized in Table 6. It is observed the formation of two peaks for PVB and most of the nanocomposites. The first peak around 60 °C can be attributed to PVB, while the second, around 84 °C, refers to PVA. According to some authors, the presence of shoulders in Tan δ curves is indicative of elevated AD. [14] This hypothesis is confirmed in this work, as PVB-MWCNT 1.0, PVB-MWCNT 0.1, PVB-GNP 0.5 and neat PVB samples, which AD values vary from 60 to 77 mol%, present two peaks in Tan δ curves. On the other hand, samples with lower AD values presented only one peak.

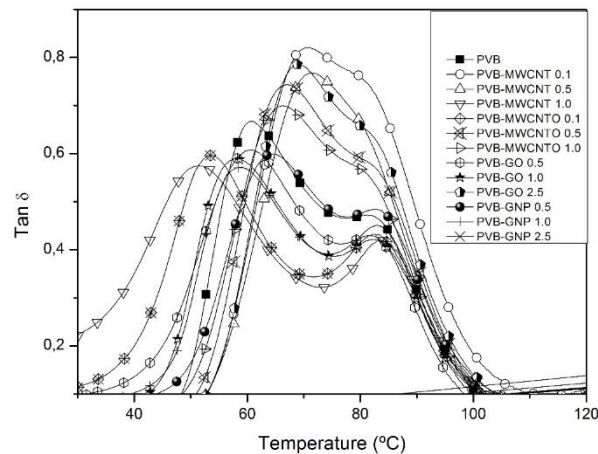


Figure 5: Curves of Tan δ vs Temperature for PVB and nanocomposites, obtained from [13, 27].

It is thus observed the formation of an immiscible PVB/PVA system for the samples with high AD values (> 60 mol%), whereas by decreasing the degree of acetalization the blend becomes miscible. In the case of the PVB-GO 2.5 wt%, for instance, the high value of T_g is probably associated with the AD value and not directly linked to the GO's action. [28]

The adhesion factor 'A' is a parameter that indicates the existence of interactions between polymer and nanoparticle, proposed by Kupta and collaborators. [31] It is defined by Equation (4), using the values of Tan δ of the nanocomposite (Tan δ_c) and the neat polymer (Tan δ_p), and the volumetric fraction of nanoparticles (α_r).

Table 6: Tg values obtained by DMA and comparative with degree of acetalization for PVB and nanocomposites.

Sample	1 st Tg (°C)	2 nd Tg (°C)	AD (mol%)
PVB	60	84	65
PVB-MWCNT 0.1	70	--	50
PVB-MWCNT 0.5	72	--	58
PVB-MWCNT 1.0	50	84	77
PVB-MWCNT 0.1	54	84	68
PVB-MWCNT 0.5	65	84	56
PVB-MWCNT 1.0	67	84	55
PVB-GO 0.5	59	84	60
PVB-GO 1.0	57	84	68
PVB-GO 2.5	70	--	51
PVB-GNP 0.5	65	84	65
PVB-GNP 1.0	57	84	66
PVB-GNP 2.5	55	84	69

Strong interactions between the reinforcement and matrix at the interface tend to reduce the macromolecular mobility in comparison with the bulk. Thus, low 'A' values indicate a high degree of interaction or adhesion between the phases [32], and the limit value for non-adhesion would be at A = 0. [33]

$$A = \frac{1}{(1 - \alpha_r)} \frac{\tan \delta_c}{\tan \delta_p} - 1 \quad (4)$$

Table 7 shows the correlation of adhesion factor and AD values with PVB and nanocomposites. Figure 6 shows the relationship between adhesion factor and AD values. Negative values for 'A' indicate that the interface has broken, while low positive values indicate significant adhesion between the nanoparticle and the polymer. [30-32]

Table 7: Adhesion factor ('A') and AD values for PVB and nanocomposite samples

Sample	'A'	AD (mol%)
PVB	--	65
PVB-MWCNT 0.1	0.24	50
PVB-MWCNT 0.5	0.15	58
PVB-MWCNT 1.0	-0.13	77
PVB-MWCNT 0.1	-0.10	68
PVB-MWCNT 0.5	0.15	56
PVB-MWCNT 1.0	0.04	55
PVB-GO 0.5	-0.07	60
PVB-GO 1.0	-0.10	68
PVB-GO 2.5	0.18	51
PVB-GNP 0.5	-0.09	65
PVB-GNP 1.0	-0.13	66
PVB-GNP 2.5	-0.10	69

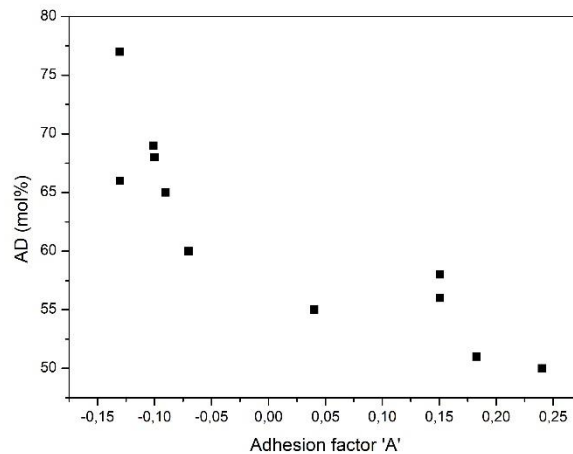


Figure 6: Relationship between adhesion factor ‘A’ and AD values.

The results show that samples with lower AD values have greater interfacial interaction between the nanoparticles and the polymer matrix. These results also agree with the C-factor. For these samples, the A and C factors indicate that the storage modulus were considerably influenced by the nanoparticles, probably due to the strong interactions between them and the vinyl alcohol groups that are still present in the PVB.

Another interesting factor is that the samples with the best results for both factors (A and C) have low AD (<60 mol%), suggesting that the presence of nanoparticles affects the synthesis of PVB (from PVA) and alters its chemical composition, but also ensured better interaction with the polymer matrix and consequently a better mechanical behavior as seen in Figure 2 and Table 3.

Figure 7 shows the Cole-Cole plots, where the loss modulus is plotted as a function of the storage modulus at a frequency of 2 Hz. These plots are reported to be indicative of the nature of the system. Homogeneous polymeric systems are reported to show a semicircle diagram, while two-phase systems show an imperfect semicircle (elliptical path). [27, 33]. On analyzing the Cole-Cole plots of PVB-matrix systems, it is mostly seen imperfect semicircles, confirming the presence of two phases, but also suggesting significant adhesion. Again, the results show that the samples with lower AD values present themselves as more homogeneous systems, with greater dispersion and interfacial interaction between the nanoparticles and the polymeric matrix, which also corroborates the results of the 'A' and 'C' factors and the from the degree of entanglement.

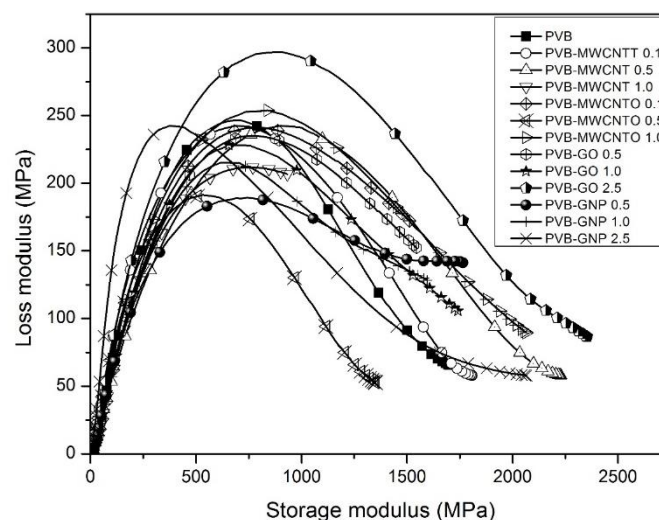


Figure 7: Cole-Cole plots for PVB and nanocomposites

3.3 Scanning electron microscopy

In Figure 8, large clusters of pristine and oxidized MWCNT, with agglomerates of almost 10 μm , can be observed in SEM images for PVB-MWCNT and PVB-MWCNTO systems. The micrographs of fracture surfaces suggest a stronger adhesion for the nanocomposites with MWCNTO. Nevertheless, in all cases, significant nanotube pull-out is observed.

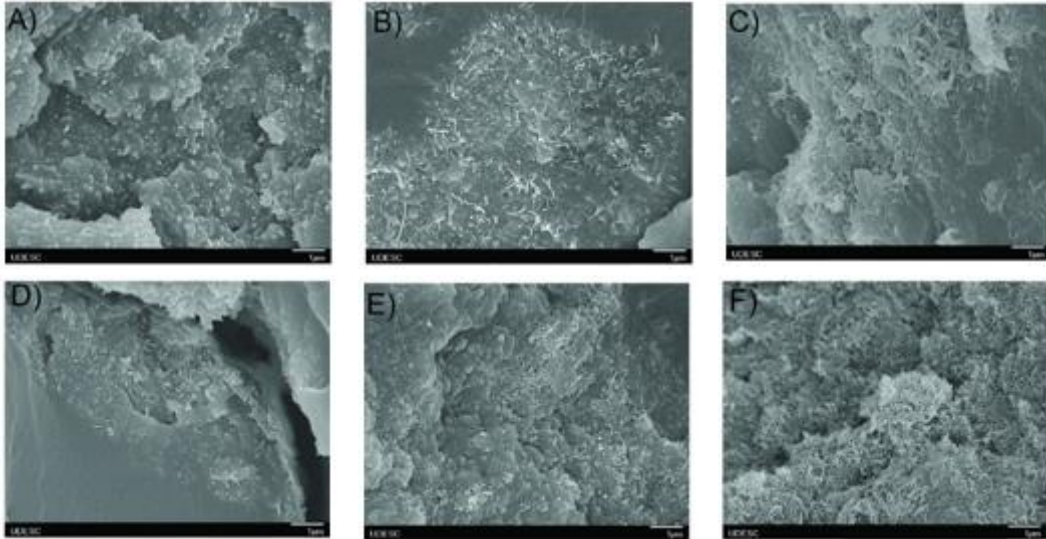


Figure 8: SEM images of nanocomposites a) PVB-MWCNT 0.1; b) PVB-MWCNT 0.5; c) PVB-MWCNT 1.0; d) PVB-MWCNTO 0.1; e) PVB-MWCNTO 0.5 and f) PVB-MWCNTO 1.0.

Considering the N and C-factors and that the systems are not very well dispersed, it is possible to conclude that increases in storage modulus values for MWCNT-nanocomposites are more dependent of the AD than to the reinforcement by carbon nanotubes.

On the other hand, the presence agglomerates is not observed for nanocomposites with GO and GNP (Figure 9). Again, the adhesion seems to be effective.

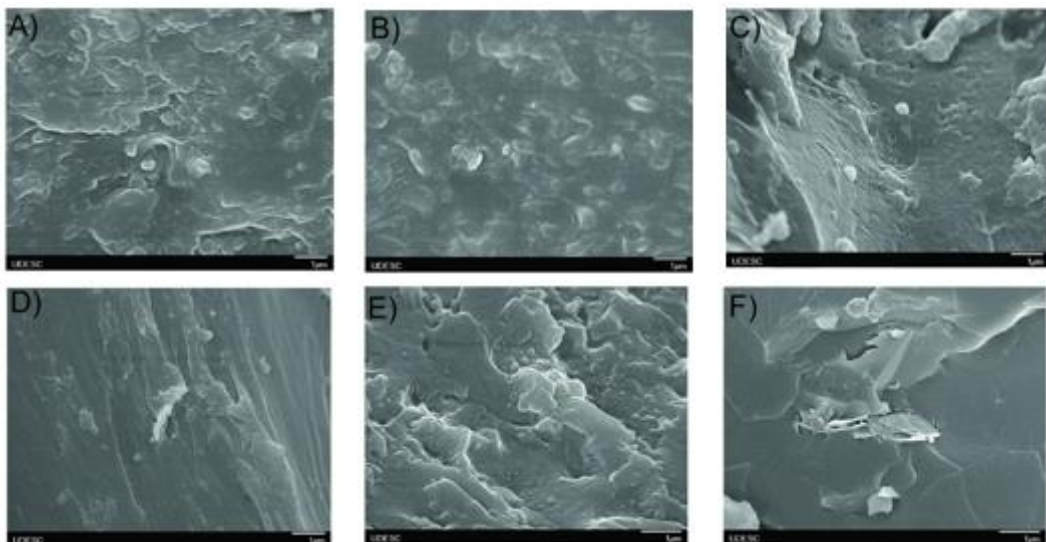


Figure 9: SEM images for nanocomposites a) PVB-GO 0.5; b)PVB-GO 1.0; c) PVB-GO 2.5; d) PVB-GNP 0.5; e) PVB-GNP 1.0 and f) PVB-GNP 2.5

5. CONCLUSIONS

PVB/nanocarbon nanocomposites have been successfully prepared by an *in situ* method, i.e. adding graphene or carbon nanotubes during PVB syntheses from PVA and butyraldehyde. Dynamic mechanical analyses showed the influences of the acetalization degree (AD) and addition of carbon nanoparticles on the storage modulus and damping factor ($\tan \delta$), as well as reinforcement efficiency (C-factor), adhesion factor and degree of entanglement. Nanocomposites with better dispersion and PVB/nanocarbon interfacial interaction presented AD values lower than neat PVB, clearly showing the dominant effect of the AD on the dynamic mechanical properties. It was also verified that the presence of nanoparticles affects the condensation reaction of PVA hydroxyl groups with butyraldehyde, changing the AD and influencing possible applications of these materials. The samples reinforced with MWCNT showed lower AD values than the samples reinforced with GO and GNP, showing that the nanoparticle geometry can also influence the acetalization reaction of PVA in PVB.

6. ACKNOWLEDGMENTS

The authors are grateful to CNPq and FAPESC by financial support and for the scholarship to J.C. Hoepfner, and CAPES by financial support and scholarship to R. C. T. Porto.

7. REFERENCES

- [1] FERNANDEZ, M.D., FERNANDÉZ, M.J., HOCES, P., ‘Synthesis of poly (vinyl butyral) s in homogeneous phase and their thermal properties’, *Journal of Applied Polymer Science*, v. 5, pp. 5007-5017, Sep. 2006.
- [2] SARAVANAN, S., GOWDA, K.A., VARMAN, K.A., *et al.*, ‘In-situ synthesized poly (vinyl butyral)/MMT-clay nanocomposites: The role of degree of acetalization and clay content on thermal, mechanical and permeability properties of PVB matrix’, *Composites Science and Technology*, v. 117, pp. 417-427, Jul. 2015.
- [3] YANG, B., LIU, R., HUANG, J., *et al* ‘Reverse Dissolution as a Route in the Synthesis of Poly(vinyl butyral) with High Butyral Contents’, *Industry Engineering Chemical Research*. v.52, pp.7425-7431, May. 2013
- [4] SALIMI, A., OMIDIAN, H., ZOHURIAAN-MEHR, M.J. ‘Mechanical and thermal behavior of modified epoxy–novolak film adhesives’, *Journal of Adhesion Science Technology*, v.17, pp. 1847-1861, Apr 2012.
- [5] KAVITA, MORDINA, B., TIWARI, R.K. ‘Thermal and mechanical behavior of poly(vinyl butyral)-modified novolac epoxy/multiwalled carbon nanotube nanocomposites’. *Journal Applied Polymer. Science*, v. 133, pp. 43333, Dec. 2015
- [6] CHAPUIS, V., PÉLISSET, P., RAEIS-BARNÉOUD, *et al.* ‘Compressive-shear adhesion characterization of polyvinyl-butyril and ethylene-vinyl acetate at different curing times before and after exposure to damp-heat conditions’, *Progress in Photovoltaics Research and Applications*, v.22, pp. 405-414, Apr. 2014.
- [7] SALMAN, SUHAD D. *et al.* ‘Ballistic impact resistance of plain woven kenaf/aramid reinforced polyvinyl butyral laminated hybrid composite’, *BioResources*, v. 11, n. 3, p. 7282-7295. Apr 2016.
- [8] RAGHAVENDRACHAR, P., CHANDA, M., ‘A kinetic model for heterogeneous acetalization of poly(vinyl alcohol)’, *European Polymer Journal*, v. 20, pp. 257-263, Dec. 1984.
- [9] LIN, XI YAN, *et al.* Process intensification of the synthesis of poly (vinyl butyral) using a microstructured chemical system. *Industrial & Engineering Chemistry Research*, v. 54, n. 14, pp. 3582-3588; Mar. 2015.
- [10] HAJIAN, M., KOOHMAREH, G.A., RASTGOO, M. ‘Investigation of factors affecting synthesis of polyvinyl butyral by Taguchi method’, *Journal of Applied Polymer Science*, v. 115, n. 6, pp. 3592-3597, Jan. 2010.
- [11] FLORY, P.J., ‘Intramolecular reaction between neighboring substituents of vinyl polymers’ *Journal of the American Chemical Society*, v. 61, n. 6, p. 1518-1521. Mar 1939.
- [12] HAJIAN, M., REISI, M.R., KOOHMAREH, A.L., *et al.*, ‘Preparation and characterization of Polyvinyl-butyril/Graphene Nanocomposite’, *Journal Polymer Research*, v. 19, Sep. 2012.
- [13] HOEPFNER, J.C., LOOS, M.R., PEZZIN, S.H. ‘Evaluation of thermomechanical properties of polyvinyl butyral nanocomposites reinforced with graphene nanoplatelets synthesized by in situ *polymerization*’ *Journal of Applied Polymer Science*, v. 135, n. 17, p. 46157, Jan. 2018.
- [14] SARAVANAN, S., *et al.* ‘Influence of mesoporous silica and butyral content on the mechanical, water absorption, and permeability properties of in situ synthesized silica/PVB nanocomposite films’, *Polymer-Plastics Technology and Engineering*, v. 55, n. 12, pp. 1220-1230, Mar. 2016.
- [15] PACHEKOSKI, W.M., AMICO, S.C., PEZZIN, S.H., *et al* (2017) Carbon nanotube hybrid polymer composites: recent advances in mechanical characterization. In: Vijay Kumar Thakur; Manju Kumari Thakur; Asokan Pappu. (Org.). Hybrid Polymer Composite Materials. 1ed.Duxford: Elsevier / Woodhead, 2017, v. 1, p. 133-150.

- [16] GEIM, A.K., NOVOSELOV, K.S., 'The rise of graphene' *In: Nanoscience and technology: a Collection of Reviews from Nature Journals*. p. 11-19.
- [17] LEE, C. *et al.* 'Measurement of the elastic properties and intrinsic strength of monolayer graphene', *Science*, v. 321, n. 5887, pp. 385-388, Jul. 2008.
- [18] YANG, X., *et al.* 'Superparamagnetic graphene oxide-Fe₃O₄ nanoparticles hybrid for controlled targeted drug carriers', *Journal of Materials Chemistry*, v. 19, n. 18, pp. 2710-2714, Mar. 2009.
- [19] SUN, Y., WU, Q., SHI, G. 'Graphene based new energy materials' *Energy & Environmental Science*, v. 4, n. 4, pp. 1113-1132, Feb. 2011.
- [20] LI, XUESONG, *et al.* 'Transfer of large-area graphene films for high-performance transparent conductive electrodes', *Nano letters*, v. 9, n. 12, pp. 4359-4363, Oct. 2009.
- [21] HUSSAIN, S., *et al.* 'Spectroscopic investigation of modified single wall carbon nanotube (SWCNT)' *Journal of Modern Physics*, v. 2, n. 06, pp. 538, Apr. 2011.
- [22] FENG, Y., *et al.* 'Room temperature purification of few-walled carbon nanotubes with high yield', *ACS Nano*, v. 2, n. 8, pp. 1634-1638, Aug. 2008.
- [23] YADAV, S.K., CHO, J.W.. 'Functionalized graphene nanoplatelets for enhanced mechanical and thermal properties of polyurethane nanocomposites' *Applied Surface Science*, v. 266, pp. 360-367, Jan. 2013.
- [24] MITTAL, G., *et al.* 'A review on carbon nanotubes and graphene as fillers in reinforced polymer nanocomposites' *Journal of Industrial and Engineering Chemistry*, v. 21, pp. 11-25, Mar. 2014.
- [25] SILVA, D.D., SANTOS, W.F., PEZZIN, S.H., 'Nanocompósitos de matriz epoxídica com reforços produzidos a partir do grafite natural'. *Matéria (Rio de Janeiro)*, v. 18, n. 2, pp. 1216-1272, May. 2013.
- [26] HOEPFNER, J.C., PEZZIN, S.H., 'Functionalization of carbon nanotubes with (3 - glycidyloxypropyl) - trimethoxysilane: Effect of wrapping on epoxy matrix nanocomposites' *Journal of Applied Polymer Science*, v. 133, n. 47, Aug. 2016.
- [27] HOEPFNER, J.C., LOOS, M. R., PEZZIN, S.H. 'Role of the degree of acetalization on dynamic mechanical properties of polyvinyl butyral/carbon nanotube composites' *Journal of Applied Polymer Science*, v. 136, p. 48146, May. 2019
- [28] POTHAN, L.A., OOMMEN, Z., THOMAS, S. 'Dynamic mechanical analysis of banana fiber reinforced polyester composites' *Composites Science and technology*, v. 63, n. 2, pp. 283-293, Jan. 2003.
- [29] HAMEED, N. *et al.* 'Morphology, dynamic mechanical and thermal studies on poly (styrene-co-acrylonitrile) modified epoxy resin/glass fibre composites' *Composites Part A: Applied Science and Manufacturing*, v. 38, n. 12, pp. 2422-2432, Aug. 2007.
- [30] OOMMEN, Z., GROENINCKX, G., THOMAS, S. 'Dynamic mechanical and thermal properties of physically compatibilized natural rubber/poly (methyl methacrylate) blends by the addition of natural rubber - graft - poly (methyl methacrylate)' *Journal of Polymer Science Part B: Polymer Physics*, v. 38, n. 4, pp. 525-536, Jan. 2000.
- [31] JYOTI, J. *et al.* 'Dynamic mechanical properties of multiwall carbon nanotube reinforced ABS composites and their correlation with entanglement density, adhesion, reinforcement and C factor' *RSC advances*, v. 6, n. 5, pp. 3997-4006, Jan. 2016.
- [32] KUBAT, J., RIGDAHL, M., WELANDER, M. 'Characterization of interfacial interactions in high density polyethylene filled with glass spheres using dynamic - mechanical analysis' *Journal of Applied Polymer Science*, v. 39, n. 7, pp. 1527-1539, Jan. 1990.
- [33] CORREA, C.A., RAZZINO, C.A., HAGE JR, E. 'Role of maleated coupling agents on the interface adhesion of polypropylene-wood composites' *Journal of Thermoplastic Composite Materials*, v. 20, n. 3, pp. 323-339, May 2007.
- [34] CHANDRA, R., SINGH, S.P., GUPTA, K. 'Damping studies in fiber-reinforced composites—a review' *Composite structures*, v. 46, n. 1, pp. 41-51, Jul. 1999.

ORCID

Jean Carlos Hoepfner	https://orcid.org/0000-0003-0933-8254
Renato César Tobias Porto	https://orcid.org/0000-0002-0206-4388
Patrícia Zigoski Uchoa	https://orcid.org/0000-0002-4483-7000
André Lourenço Nogueira	https://orcid.org/0000-0003-4162-5472
Sérgio Henrique Pezzin	https://orcid.org/0000-0002-5667-1968